Paper ID: IM-16-12432

Title: Measurement of the Mass Flow and Velocity Distributions of Pulverized Fuel in Primary Air Pipes Using Electrostatic Sensing Techniques

Authors: Xiangchen Qian [a]

Yong Yan [b] (Corresponding author)

Xiaobin Huang [a]

Yonghui Hu [a]

Addresses: [a] School of Control and Computer Engineering

North China Electric Power University

Beijing, 102206

P. R. China

[b] School of Engineering and Digital Arts

University of Kent

Canterbury,

Kent CT2 7NT

UK

Tel: 00441227823015

Fax: 00441227456084

Email: y.yan@kent.ac.uk

ABSTRACT

On-line measurement of pulverized fuel (PF) distribution between primary air pipes on a coal-fired power plant is of great importance to achieve balanced fuel supply to the boiler for increased combustion efficiency and reduced pollutant emissions. An instrumentation system using multiple electrostatic sensing heads are developed and installed on 510 mm bore primary air pipes on the same mill of a 600 MW coal-fired boiler unit for the measurement of PF mass flow and velocity distributions. An array of electrostatic electrodes with different axial widths is housed in a sensing head. An electrode with a greater axial width and three narrower electrodes are used to derive the electrostatic signals for the determination of PF mass flow rate and velocity, respectively. The PF velocity is determined by multiple cross-correlation of the electrostatic signals from the narrow electrodes. The measured PF velocity is applied on the root-mean-square magnitude of the measured electrostatic signal from the wide electrode for the calibration of PF mass flow rate. On-plant comparison trials of the developed system were conducted under five typical operating conditions after a system calibration test. Isokinetic sampling equipment is used to obtain reference data to evaluate the performance of the developed system. Experimental data demonstrate that the developed system is effective and reliable for the on-line continuous measurement of the mass flow and velocity distributions between the primary air pipes of the same mill.

Index Terms–Pulverized fuel, fuel distribution, fuel velocity, power plant, electrostatic sensor, gas–solid two-phase flow.

I. INTRODUCTION

About 40% of the electricity in the world was generated from coal in 2014, and the demand of coal for power generation will increase 2.1% annually in the coming five years [1]. However, coal-fired power plants face challenges to enhance energy conversion efficiency and to produce less pollutant emissions. Instrumentation and measurement techniques have an important part to play to combat the above challenges. On-line measurement of the mass flow rate and velocity of pulverized fuel (PF) in a fuel injection pipeline is of primary importance for the control of fuel transportation, balancing fuel distribution between primary air pipes, and optimization of the combustion process.

The on-line measurement of PF has been recognized as a long-standing industrial problem because the PF particles in a primary air pipe are very dilute with a volumetric concentration of less than 0.1% and are inhomogeneously distributed in the pipe with a highly irregular velocity profile. Very few sensing techniques are available to cover the whole cross-section of a primary air pipe with a diameter ranging from 400 mm to 650 mm. Therefore, instruments based on ultrasonic, microwave and imaging techniques have never performed satisfactorily on power plants in a longer term due to their inherent limitations in sensing principles and applicability [2].

Electrostatic induction based ring-shaped sensors offer a promising solution to the measurement problem due to its advantages for industrial use, such as robustness in a harsh environment, non-intrusiveness in installation, no energy injection to the flow, large cross-sectional sensing volume, good affordability and low maintenance requirements [3]. The electrostatic sensing principle in combination with cross-correlation signal processing method for the velocity measurement of pneumatically conveyed particles have been well studied for over three decades [4]–[6]. The latest research on the electrostatic sensing based particle cross-correlation velocimetry [7]–[9] provides a reliable solution to the PF velocity measurement.

Substantial effort has been made to relate the characteristics of electrostatic signals from various types of electrostatic sensors to the mass flow rate of pneumatically conveyed particles through both laboratory tests [4]-[6], [10]–[14] and industrial trials [14]–[16]. The root-mean-square (rms) magnitude (rms charge level) of an electrostatic signal is used as an indication of the volumetric concentration of particles under steady, dilute-phase flow conditions [11]–[16]. Gajewski suggested that the rms value of an electrostatic signal can be used to directly measure the mass flow rate of polyvinyl chloride (PVC) dust over the velocity range below 20 m/s if the effect of particle velocity has been compensated [5]. Zhang proposed a theory that the rms charge level of pneumatically conveyed fillite particles and its mass flow rate have a second order polynomial relationship when the air-to-solids ratio between 1.92 and 3.86 [14]. Qian *et al* developed an arc-shaped electrostatic sensor array based PF flow monitoring system for on-line measurement of fuel particle velocity and fuel mass ratio among the fuel pipes of the same mill [15]. Jurjevčič *et al* used a matrix of rod electrostatic sensors to determine the mass flow distribution in the cross-section of a duct that feeds the pulverized lignite to four burner nozzles by measuring the transferred electrostatic charge and velocity of PF particles [16]. However, it is still challenging to develop a reliable and robust system that is operational on a full-scale power plant because the above techniques require complicated calibration testing or provide localized and intrusive measurement.

In this study, an instrumentation system comprising five independent electrostatic sensing heads and a central data analysis station was designed, implemented and installed on 510 mm bore primary air pipes from the same pulverizing mill of a 600 MW coal-fired boiler unit. An array of electrodes that consists of three narrow electrodes and one with a much wider axial width is proposed to measure the PF velocity and flow rate based on their advantages of wider sensing signal bandwidth, better spatial filtering effect and a larger sensing volume, respectively. Comparison trials of the developed system were conducted under five distinct flow test conditions for the measurement of mass flow and velocity distributions between different PF feeding pipes of the same mill. There are currently no reliable

systems in operation for the intended measurement in power stations. There are also no established measurement standards in industry. The isokinetic sampling is probably the only commonly accepted reference for the validation of a new PF flow measurement system under test. Isokinetic sampling equipment was used in this study to obtain reference data and evaluate the system under development. Preliminary experimental results were presented at the 2016 International Instrumentation and Measurement Technology Conference [17]. This paper describes in detail the design, implementation and evaluation of the measurement system along with comprehensive experimental results and interpretations under a wider range of test conditions.

II. MEASUREMENT PRINCIPLES

In a coal-fired power plant, bulk coal is pulverized into fine particles and then pneumatically conveyed towards a matrix of burners via a primary air pipe network. PF particles become electrically charged during pneumatic transportation in primary air pipes [5], [6]. Electrostatic sensors, which are passive (i.e., no injection of energy in any form to the flow), make good use of the electrostatic phenomenon to measure the PF flow. As the charged particles move through the sensor, induced electrostatic charge will appear on its surface [5], [6].

A. Principle of PF Velocity Measurement

As an indication of volumetric concentration (β_s) of PF particles, the rms charge level is more sensitive to the particle velocity than the mass flow rate and other parameters [5],[6],[11]–[15]. Thus, the accurate measurement of the particle velocity is vital for mass flow rate measurement. Fig. 1 shows the basic principle and structural design of the latest model of the PF flow measurement system. As can be seen from Fig. 1, three identical narrow electrodes and one wider electrode are housed in a sensing head to measure the flow parameters of the PF. The narrow electrodes, which yield a wider signal bandwidth, are used to measure the PF velocity using two parallel electrodes through cross-correlation velocimetry [5], [12], [15]:

$$v_{ij} = \frac{(i - j)L}{\tau} \tag{1}$$

where i, j = 1, 2 or 3, L is the center-to-center spacing between two adjacent electrodes. The transit time taken by PF particles to move from the upstream electrode i to the downstream electrode j is determined from the location of the dominant peak (correlation coefficient r_{ij}), i.e., in the cross-correlation function [15]. Since the spacing between the two corresponding electrodes is known, the individual PF velocity is then derived.

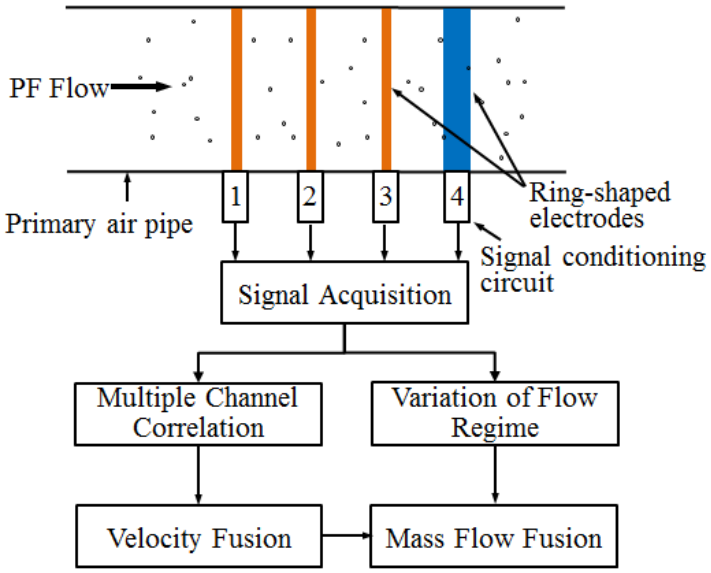

Fig. 1. Structure and principle of the measurement system.

The use of three narrow electrodes is a trade-off between fast system response, measurement reliability and compactness of the sensing head. The weighted average PF velocity (v_c) is determined by fusing the three individual velocities:

$$v_c = \frac{r_{12}v_{12} + r_{23}v_{23} + r_{13}v_{13}}{r_{12} + r_{23} + r_{13}}. \tag{2}$$

In practical, r_{13} is much lower than r_{12} and r_{23} due to the ever-changing flow regime and the longer spacing between electrodes 1 and 3. Thus, v_{13} is not calculated in most cases when the difference between v_{12} and v_{23} is reasonable. Such strategy shortens the response time of the system without

compromise of the measurement precision. In this case the weighted average PF velocity is than derived as

$$v_c = \frac{r_{12}v_{12} + r_{23}v_{23}}{r_{12} + r_{23}}. \tag{3}$$

When the correlation coefficients are greater than a specific value (e.g. 0.4) and the difference between v_{12} and v_{23} is greater than 3 m/s, v_{13} is calculated as a reference with previous v_c to compare with v_{12} and v_{23}. The one that has less and reasonable difference with both references is selected to represent the PF velocity. When PF flow regime fluctuates significantly, there will be less than 1% possibility (in this study) that the value of calculated correlation coefficients (r_{12} and r_{23}) are lower than 0.3 and the measured PF velocities (v_{12} and v_{23}) do not agree with each other. In such rare cases, a measurement failure is recognized and the measurement results are regarded as invalid. The possibility of measurement failure is affected by the performance of the milling system, coal properties etc.

B. Principle of PF Mass Flow Rate Measurement

The wide electrode, which has a larger sensing volume and better spatial filtering effect [4]–[6], is applied to infer the volumetric concentration of PF. The mass flow rate of PF particles is derived from [6], [11]:

$$q_{m,s} = A_p \rho_s v_c \beta_s \tag{4}$$

where A_p is the cross-sectional area of the pipe and ρ_s the true density of the fuel. As the rms charge level of the electrostatic signal (A_{rms}) is an indication of the volumetric concentration of PF particles [6], [11], [12], [14], [15], the mass flow rate of PF particles is calculated from the rms charge level from the wide electrode and the cross-sectional averaged velocity of PF measured from the narrow electrodes:

$$q_{m,s} = a v_c^b A_{rms} \tag{5}$$

where a is a proportionality coefficient that mainly relates to fuel properties and coefficient b represents the dependence of the rms value on particle velocity and variation of flow regime. Coefficients a and b are determined through a calibration process using isokinetic sampling equipment [15]. Since the properties of PF particles in the pipes from the same pulverizing mill are very similar, the fuel distribution between the primary air pipes of the same mill is presented by the percentage share of each individual mass flow rate normalized to the total mass flow rate of that mill. The fuel distribution ratio of primary pipe Ci with reference to the overall mass flow rate is determined from

$$Ratio_{Ci} = \frac{q_{m,s,Ci}}{\sum_{k=1}^{n} q_{m,s,Ck}} \tag{6}$$

where $i=\{1, 2, 3,\ldots, n\}$, $q_{m,s,Ci}$ is the PF mass flow rate in Ci and n is the total number of primary pipes of the mill. Substituting equation (5) into equation (6), we can then calculate the fuel distribution ratio:

$$Ratio_{Ci} = \frac{v_{c,Ci}^{b} A_{rms,Ci}}{\sum_{k=1}^{n} v_{c,Ck}^{b} A_{rms,Ck}}. \tag{7}$$

C. Principles of Signal Processing and System Communication

Fig. 2 represents the simplified hardware block diagram of the measuring system. A dedicated embedded electronic circuit is used for the conditioning and processing of the electrostatic signals from the sensing head. Fig. 3 shows the schematic diagram of the signal conditioning circuit for one of the electrodes. As can be seen from Fig. 3, the weak current signal from the electrode is transformed to a voltage form through a feedback resistor (R_1) with a resistance in the order of mega ohms. As the charge density of PF particles is as low as 10^{-7} C/kg [6], the selection of the feedback resistor is essential to keep signals from severe distortion and to reach an appropriate magnitude for subsequent processing. A programmable secondary amplifier with its gain controlled by R_3 is adopted to adjust the amplitude of the pre-amplified signal to an adequate range according to the range of the PF mass flow

rate, type of coal and environmental conditions. Then the voltage signal passes through a second-order low-pass filter to eliminate high-frequency noise as well as for the purpose of anti-aliasing.

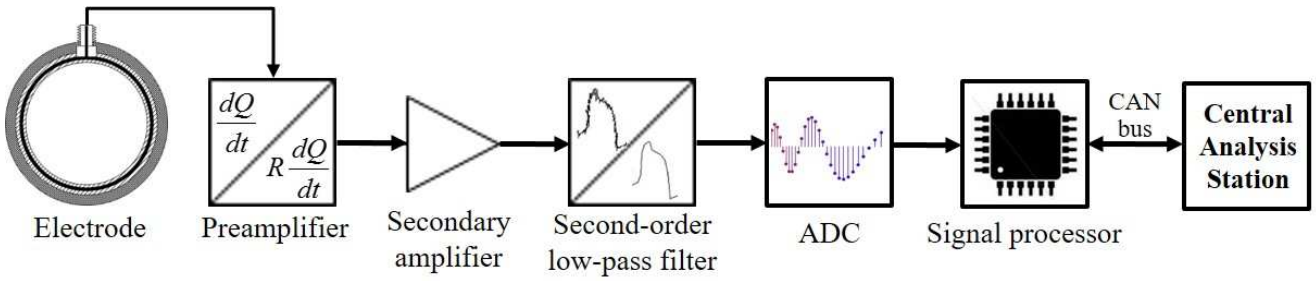

Fig. 2. Hardware block diagram of the measuring system.

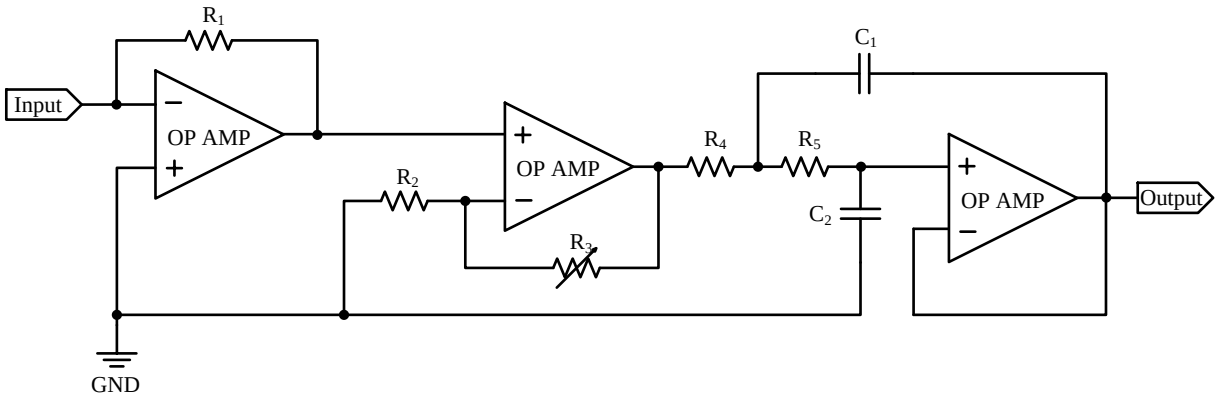

Fig. 3. Schematic diagram of the signal conditioning circuit.

The analog signals are then converted into a digital form via an analog-to-digital convertor (ADC), as shown in Fig. 2. A fast-speed, multi-functional, digital signal controller (DSC), named dsPIC® from Microchip®, is used as the core of the electronic circuit. The in-chip ADC is configured to synchronous sampling mode for data acquisition of four channels of signals. The synchronous sampling is ideal for the cross-correlation calculation because there is no time delay between the sampled signals from different channels in each sampling process. The sampling rate of the ADC is configured at 50 kHz with a 10-bit resolution. Two thousands sampling points are used for the determination of PF flow parameters in each measurement within 0.2 second. The built-in controller area network (CAN) interface was adopted to transmit the flow parameters determined by each sensing head to a local central data analysis station, as shown in Fig. 4. The use of CAN bus not only provides a reliable and

flexible way of communication between central data analysis station and each sensing head but also enables connections of up to 255 sensing heads in the system without interruption. The PF flow parameters of all the primary air pipes from the same mill are post processed in the central analysis station by smoothing and fusion algorithms to stable measurement results as well as fuel distribution between pipes. The central data analysis station is also used to adjust the operation parameters of the sensing heads according to the variation of PF flow. The measurement results are sent to the distributed control system (DCS) of the power plant for automated control of the mill and fuel supply system, for example, to adjust the dumpers for balanced fuel distribution.

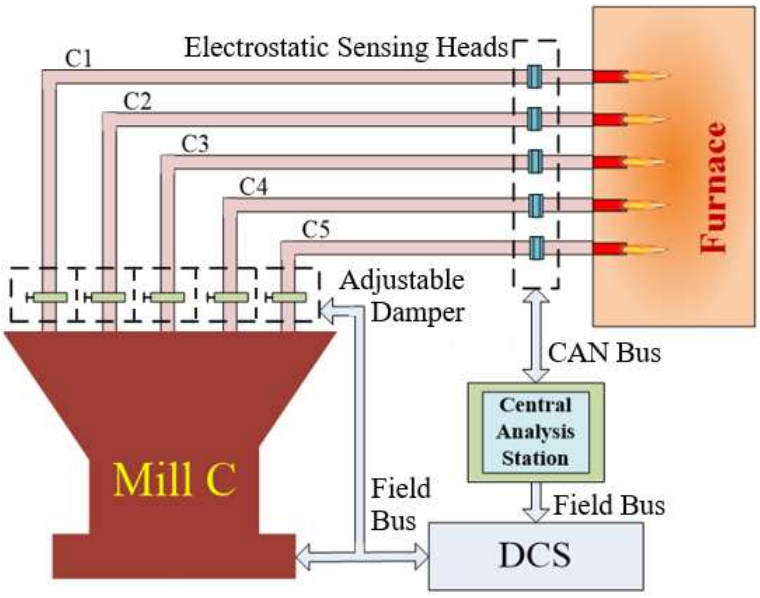

Fig. 4. Layout of the instrumentation system on a primary air pipe system.

III. System Implementation and Installation

Fig. 5 shows the implementation and installation of the sensing heads on the 510 mm bore primary air pipes of the pulverizing mill of a 600 MW boiler unit. An array of ring-shaped electrodes that consists of three identical narrow electrodes and one wider electrode is embedded in a stainless steel sensing head base and insulated from PF flow using wear-resistant insulation material. The center-to-center spacing between the two adjacent narrow electrodes is 24 mm. The axial width of the narrow electrodes is 3 mm while the wide electrode has an axial width of 40 mm. The inner surface of the sensing head is

made flush with the inner pipe wall so that a sensing head can be embedded in the primary air pipe (with flange connection) without any impact on the PF transportation system. The weak electrostatic signals are transmitted to a signal processing circuit using independent screened cables with Threaded Neill-Concelman (TNC) connectors on both sensing head and signal conditioning and processing circuits. The electronic circuit is enclosed in a grounded metal box to prevent the weak electrostatic signal from the interference of electromagnetic noise in an industrial environment.

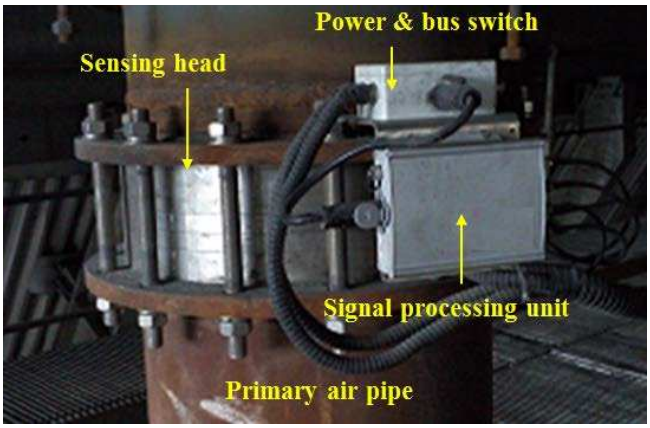

(a) Sensing head with the signal processing uint.

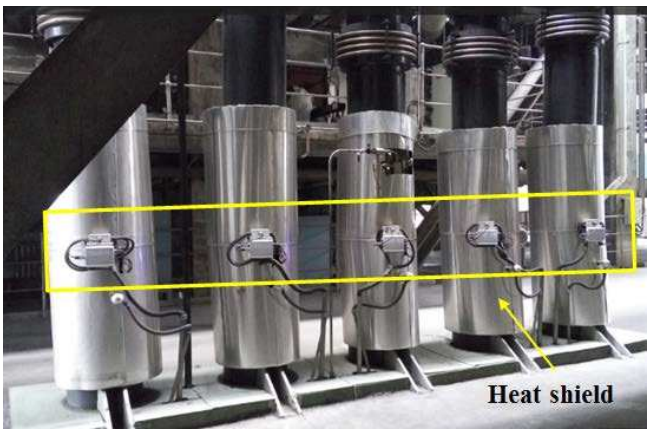

(b) Five sensing heads on the same mill (with heat insulating shield).

Fig. 5. Installation of the PF measurement system.

Four channels of typical output signals of a signal conditioning circuit are plotted in Fig. 6. As can be seen the three channels of output signals originally measured by the narrow electrodes have very similar waveforms with a small time delay. The signals measured by the wide electrode have a greater amplitude with a much longer time delay compared to those of the narrow electrodes.

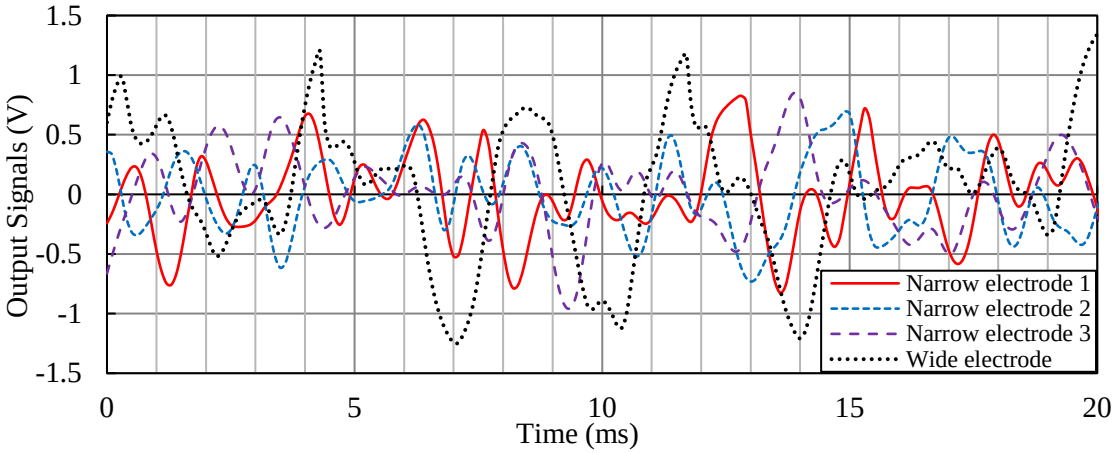

Fig. 6. Typical output signals from a signal conditioning circuit.

Because the voltage drop on a power supply cable can be considerably high, the power supply for the electrostatic system should take consideration of the overall length of the power cable and the maximum current to ensure the line voltage applies to the furthest end can meet the requirement of the signal processing circuit. In order to determine fuel distribution between the PF pipes from the same mill, all the mechanical and electrical components of the sensing heads are made identically to each other. Fig. 5(b) shows the installation of the five sensing heads on the primary air pipes of mill C at the power plant. The installation process of the sensing heads were undertaken during the shutdown of the corresponding milling system as a small section of the pipe had to be cut out. A sensing head is clamped in the primary air pipe using two flanges (welded on a primary pipe) with 16 screw rods. The heat shield is applied to cover the sensing heads and pipes for energy saving. Another benefit of the heat shield is to prevent the inner surface of an electrostatic sensing head from the adhesion of large amount of PF particles when the moisture content of PF is high.

IV. Measurement Results and Discussion

A. System Calibration Tests

System calibration tests were undertaken on primary air pipe C1 under six different conditions, as summarized in TABLE I, in prior to comparison trials.

TABLE I. CALIBRATION TEST PROGRAM

Test Conditions	Test Stages					
	i	ii	iii	iv	v	vi
PF Mass Flow (t/h)	8.0	8.0	8.0	8.0→9.0	9.0	7.0
Air Velocity (m/s)	23.8	21.4	26.0	26.0→23.6	23.6	23.6

The mass flow rate of PF and primary air velocity in the pipe were imposed by the DCS and kept steady during each test stage. The coefficient *b* in equation (5) was derived for the measurement data from the developed system and the flow parameters measured by the isokinetic sampling equipment with a measurement accuracy of ±10%. With the use of the isokinetic sampling equipment, as shown in Fig. 7 and Fig. 8, the PF mass flow rate was obtained for 15 seconds at each of the 49 sampling points over the cross-section of the pipe. The total duration of collecting the data over the pipe cross section was about 15 mins.

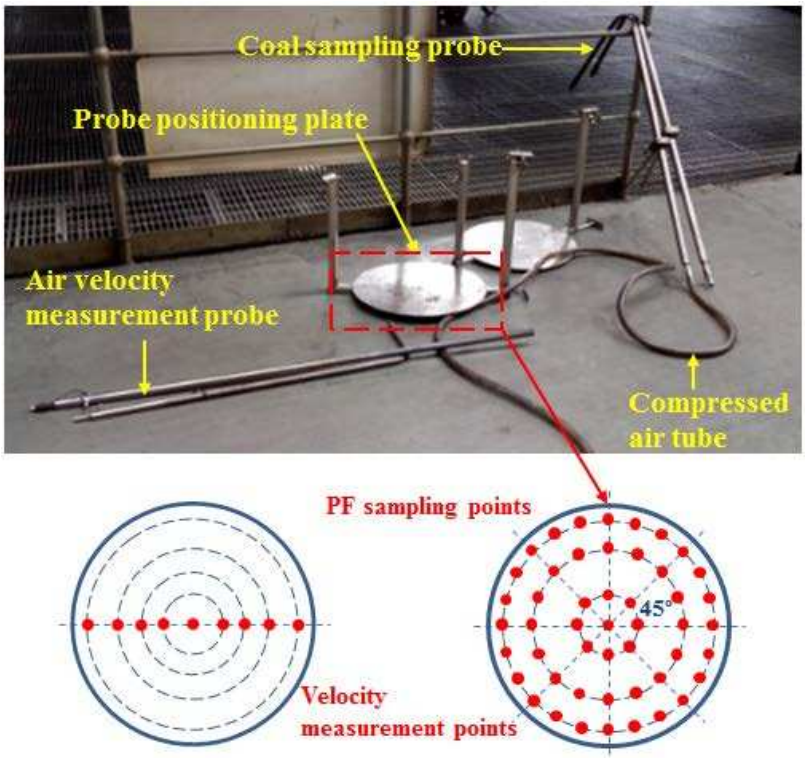

Fig. 7. Isokinetic sampling equipment.

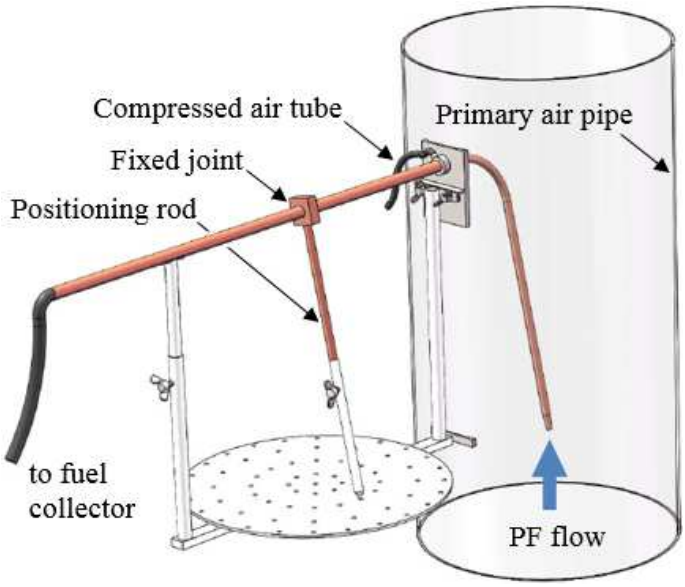

Fig. 8. Diagrammatic sketch showing the isokinetic sampling process.

Compressed air with about 0.5 MPa pressure was injected into the primary air pipe through the PF sampling port to avoid leakage of PF particle to the environment. The cross-sectionally averaged velocity of the primary air was derived based on the air velocities measured at ninth points across the diameter of the pipe cross-section using combined Pitot tube and static tube (with ±5% measurement accuracy) that measures total and static pressures. The primary air velocity v_a is derived from the following equation:

$$v_a = 3.1\sqrt{\frac{P}{\rho_a}} \tag{8}$$

where P and ρ_a are the dynamic pressure and the density of the primary air, respectively.

Fig. 9 shows the measured PF velocity, rms charge level and mass flow rate using the developed system (during a selective period of time in each test stage), along with the primary air velocity and PF mass flow rate measured from the isokinetic sampling equipment. Fig. 9(a) compares the conveying air velocity with PF velocity. It is evident that the PF velocity is consistent with the trend of the air velocity. The variation of PF mass flow rate has less effect on the PF velocity than that of air velocity because the volumetric concentration of PF in the two-phase flow is as dilute as about 0.05%. The averaged slip velocity between the PF and the conveying air in each test stage is between 0.79 m/s and

1.71 m/s and the maximum relative deviation between them is 4.73%. As shown in Fig. 9(b), the rms charge level fluctuates when either the PF mass flow rate or air velocity changes. When either of the two factors is fixed, the rms charge level follows the variation trend of the other. In the short transition stage iv, the rms charge level is steady as the PF mass flow rate and air velocity vary contrarily. The measured PF mass flow rate using equation (5) matches closely the PF mass flow rate obtained from the isokinetic sampling equipment with a mean relative error of less than 2.54%.

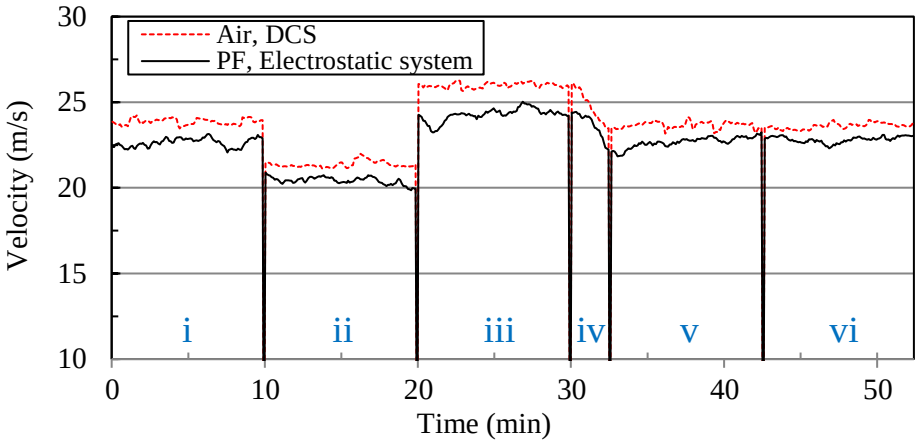

(a) Air velocity and measured PF velocity

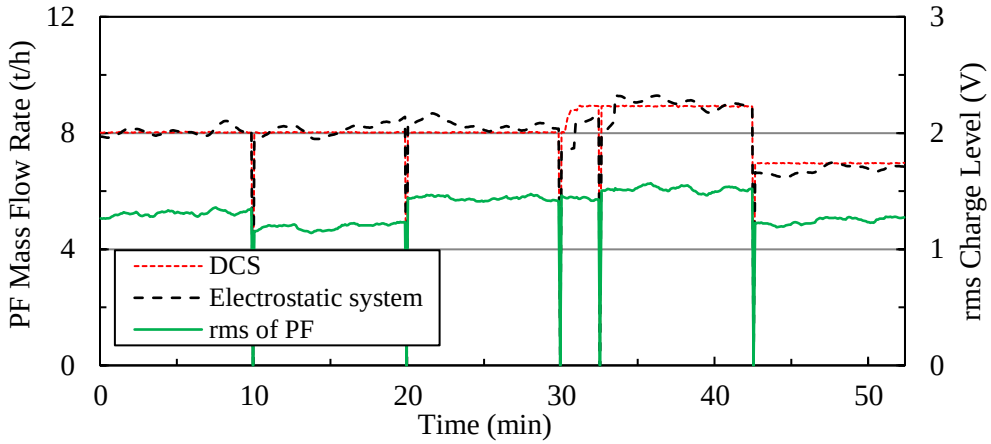

(b) PF mass flow rate with corresponding rms charge level

Fig. 9. Test results for variable PF and air flow rates.

B. Comparison Trials

The comparison trials on five primary air pipes of mill C were undertaken using the developed instrumentation system and the isokinetic equipment under five different flow conditions (TABLE II). The uniformity index of PF particles N_p is defined as:

$$N_p = \frac{\log_{10}(\ln \frac{100}{R_{200}}) - \log_{10}(\ln \frac{100}{R_{90}})}{\log_{10} \frac{200}{90}} \quad (9)$$

where, R_{90} and R_{200} represent the percentage of PF particles with an equivalent diameter greater than 90 μm and 200 μm, respectively. The value of N_p is normally in the range between 0.8 and 1.3. A greater value of N_p entails higher uniformity. The mass flow rates of air and PF were both set constant in the DCS of the plant during each trail stage. In the first three trial stages, the PF mass flow rate was fixed and the air flow rate increased from 90 t/h to 110 t/h. Then, the air flow rate was set to 100 t/h, while PF mass flow rate changed from the highest fuel load (45 t/h) to the lowest (35 t/h).

TABLE II. TEST PROGRAM FOR COMPARISON TRIALS

Test Conditions	Trial Stages				
	(a)	(b)	(c)	(d)	(e)
PF Mass Flow (t/h)	40	40	40	45	35
Air Mass Flow (t/h)	90	100	110	100	100
Mass Flow Ratio of Air to PF	2.25	2.50	2.75	2.22	2.86
R_{90} (%)	19.4	19.8	24.0	21.6	21.3
R_{200} (%)	2.3	2.9	2.6	2.4	2.4
N_p	0.98	1.05	1.14	1.10	1.09

Fig. 10 shows the measured PF velocity and rms charge level using the electrostatic system during a selective period of time in each trial stage, along with the mass flow rates of primary air and PF recorded in the DCS, respectively. Fig. 10(a) shows the measured PF velocity from the electrostatic system and the corresponding air mass flow rate. It is obvious that the PF velocities of all five primary air pipes are consistent with the trend of the air flow rate. However, the difference in PF velocity between the primary air pipes varies in different conditions. The PF velocity of pipe C5 is constantly slower than those in other pipes during the whole trial. While the PF velocity of pipe C1 is greater than those of other pipes in most cases, except a similar value is measured on pipe C3 in trail stage (a). The

PF velocities in pipes C2 and C4 are similar and slightly lower than that in pipe C3, except trial stage (b). The differences in averaged PF velocity between pipes C1 and C5, from trail stages (a) to (e), are 3.4 m/s, 3.18 m/s, 1.94 m/s, 2.4 m/s and 3.12 m/s, respectively. The ascending order of them according to each corresponding trail stage is (c), (d), (e), (b) and (a), which is the same as the order of N_p (TABLE II). As shown in Fig. 10(b), the rms charge level increases with the mass flow rates of both air and PF. The rms charge level of pipe C5 is constantly lower than those of other pipes. The order of rms charge level of pipes C1 to C4 varies in different trial stages. Such phenomenon indicates that the fuel distribution between the five pipes changes with air to PF mass flow ratio.

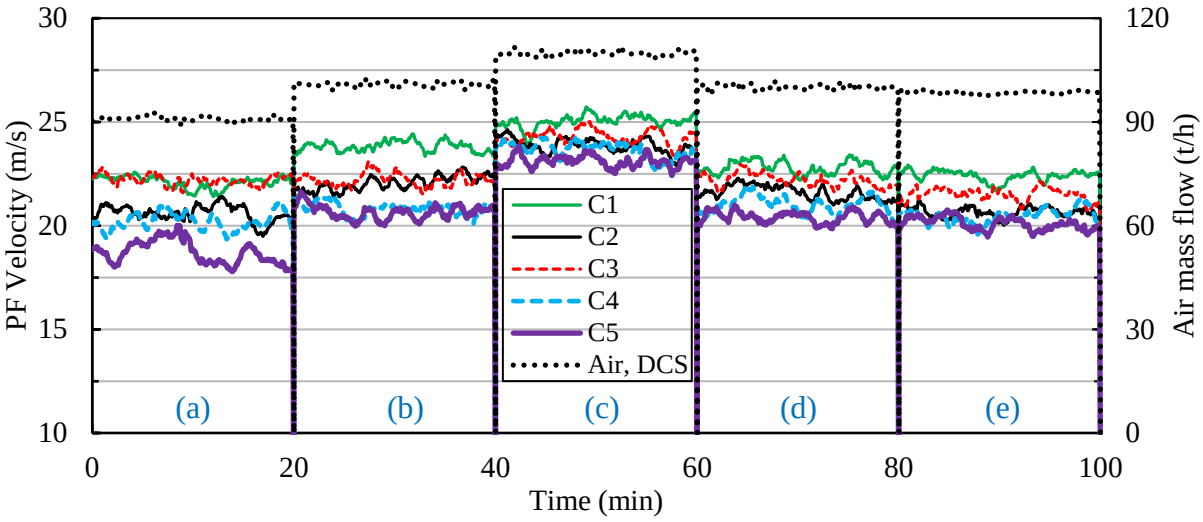

(a) Measured PF velocity and Air mass flow rate

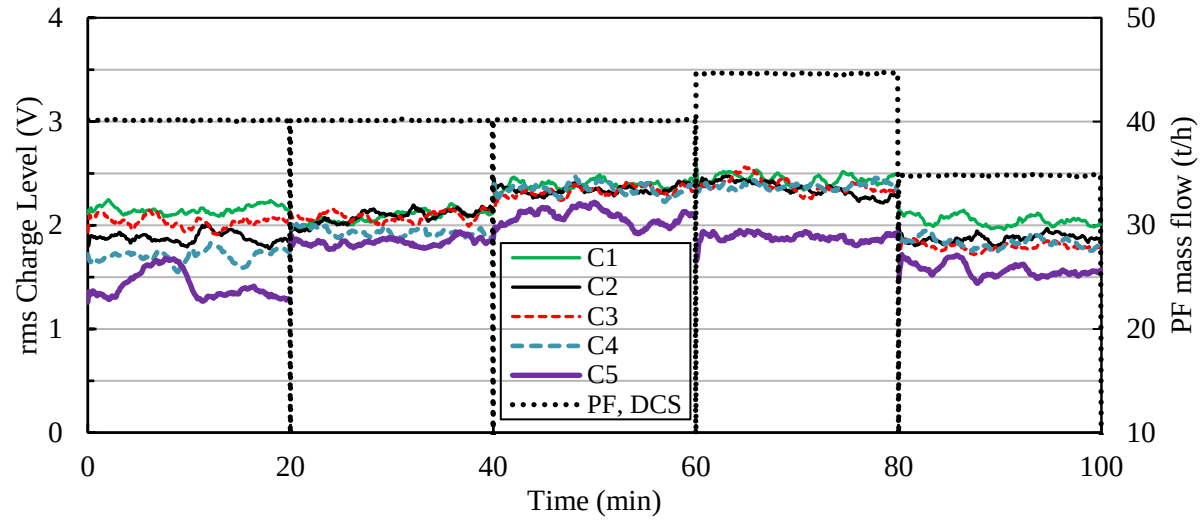

(b) Measured PF velocity and Air mass flow rate

Fig. 10. Comparison of PF parameters under different flow conditions.

The measured velocities of PF and primary air using the electrostatic system and Pitot tube, respectively, with their relative discrepancy and the standard deviation of the PF are illustrated in Fig. 11.

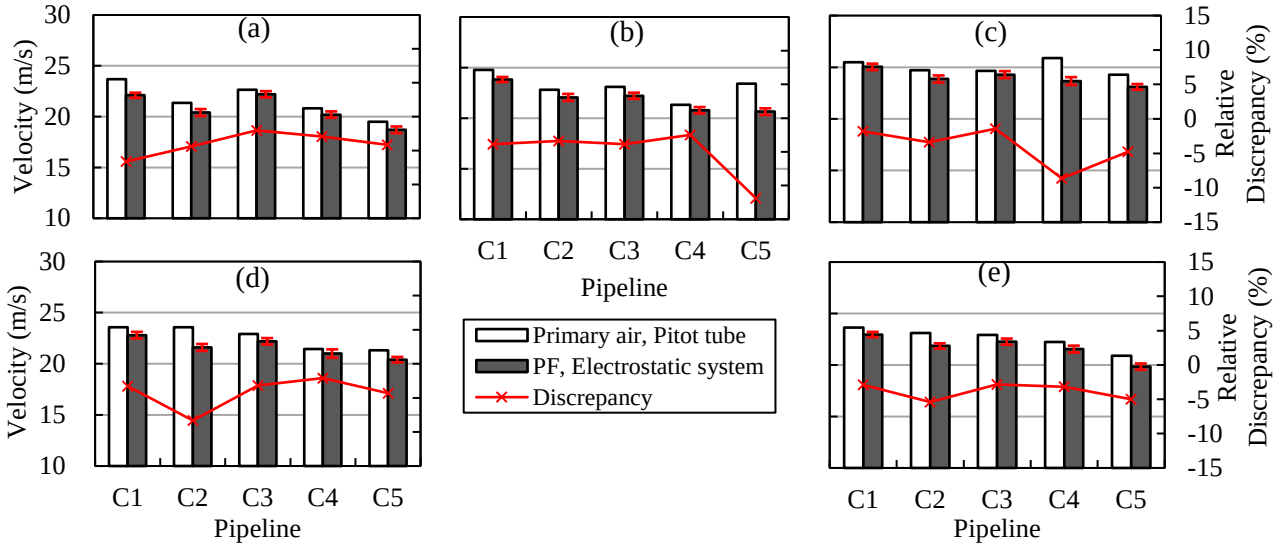

Fig. 11. Comparison of the measured PF velocities in the five pipes under different flow conditions.

It is evident that the ordinal relations of PF velocities in the five primary air pipes determined by the two methods agree with each other in most cases. The proposed system also shows good repeatability in velocity measurement under fluctuating flow conditions as the standard deviation of the velocity measurement is within the range of 0.25 m/s to 0.41 m/s, which is equivalent to a relative error of 1.1% to 1.9%. The Pitot tube is usually used for gas flow measurement, so its long term use for the measurement of particle-laden flow can significantly affect the measurement accuracy since particles get into the tube. Therefore, the discrepancy between the highest and the lowest PF velocities in the five pipes (4.2 m/s, 3.5 m/s, 1.6 m/s, 2.4 m/s and 2.8 m/s) measured from the system is greater than that from the electrostatic system (3.5 m/s, 3.2 m/s, 1.9 m/s, 2.4 m/s and 3.1 m/s). As the PF particles are motivated by the primary air, the air velocity is higher than that of PF particles in most cases (the pipe section after an elbow is an exception). The slip velocity between the air and PF particles ranges from 0.36 m/s to 2.78 m/s with an averaged slip velocity of 0.98 m/s. The relative discrepancy in the PF velocity measurement between the two methods is within ±5% in most cases. The averaged absolute

deviations of the PF velocities in pipes C1 to C5 in the five trial stages are 3.7%, 4.9%, 2.7%, 3.9% and 6.0%, respectively. It can also be seen from Fig. 11 that the FP velocity is largely affected by the mass flow rate of air but not that of PF as the flow is very dilute. Furthermore, the relationship between the PF velocities in the five primary air pipes changes more with the air mass flow rate rather than the PF flow rate as the relationship of the five velocities changes less under trial conditions (b), (d) and (e) (the same primary air mass flow rates) than those under trial conditions (a), (b) and (c) (different primary air mass flow rates).

The averaged values of the air and PF velocities measured using the two different methods under the five different air flow rates are summarized in TABLE III. The calculated air velocity is derived from the mass flow rate, pressure, temperature and humidity of the primary air with the diameter of the pipe. Both of measured air and PF velocities are consistent with the trend of the air flow rate.

TABLE III. AIR FLOW RATE AND CORRESPONGDING AIR AND PF VELOCITIES

Measurement Results	Trial Stage				
	(a)	(b)	(c)	(d)	(e)
Air Flow Rate (t/h)	90	100	110	100	100
Calculated Air Velocity (m/s)	21.4	23.8	26.0	23.8	23.8
Averaged Air Velocity (m/s)	21.6	23.1	25.0	22.6	22.5
Averaged PF Velocity (m/s)	20.7	21.9	24.0	21.6	21.6

The normalized relative discrepancy of the parameters in TABLE III with reference to that of trail stage (b) are shown in Fig. 12. The normalized relative discrepancies of the measured PF velocity in trail stages (d) and (e) are -0.8% and -1.4%, respectively, while that of the measured air is -2.3%. The results demonstrate that the measured PF velocity shows better consistency than the measured air velocity under the same air flow rate conditions (trail stages (b), (d) and (e)). When the air flow rate varies 10% in stages (a) and (c) with reference to stage (b), the measured PF and air velocities also increase in stage (a) and decrease in stage (c), accordingly.

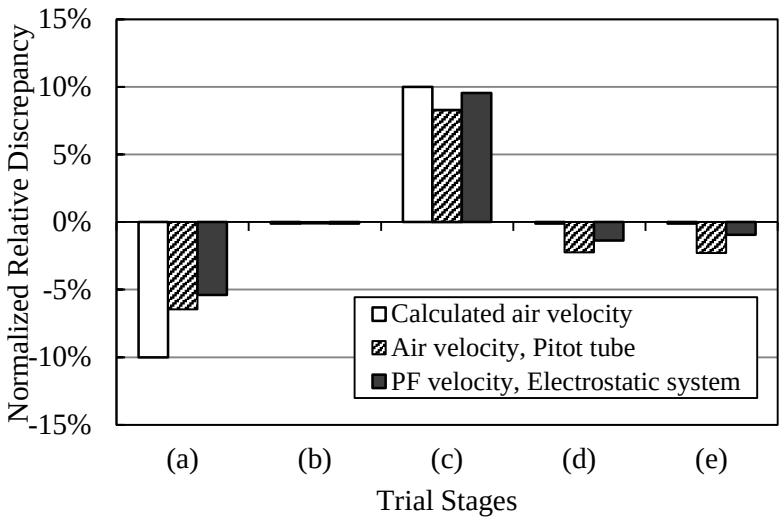

Fig. 12. Normalized relative discrepancy between the primary air flow rate and averaged PF and air velocities with reference to trial stage (b).

The measured PF mass flow distributions in the five pipelines using the two different methods are illustrated in Fig. 13. The proportional relations of PF in the five primary air pipes determined from the developed system and the isokinetic sampling equipment are very similar under all five trail stages. Due to the difference in measurement principles and practical operation between the two methods, the discrepancy between the highest and the lowest distribution ratio (8.0%, 7.4%, 7.8%, 9.6% and 7.7%) measured from the isokinetic sampling equipment is greater than that from the electrostatic system (5.2%, 3.7%, 5.0%, 6.9% and 2.4%). The relative discrepancy in mass flow distribution measurements between the electrostatic system and the isokinetic sampling equipment is less than ±15% for any pipe under any conditions. The averaged absolute deviations of mass flow distribution for pipes C1 to C5 in five trial stages are 7.9%, 8.8%, 8.2%, 10.2% and 8.9%, respectively, while the averaged absolute deviations of all the pipes are 8.7%, 9.8%, 7.3%, 9.0% and 9.3%, respectively. Such results indicate that the developed system has a good repeatability (the standard deviation is between 1.2% and 2.9%) and performs well under all trail conditions with reference to the isokinetic sampling method. Similar to the PF velocity, the PF distribution between the five primary air pipes is also mostly affected by the primary air mass flow rate as the PF distributions under trial conditions (a), (b) and (c) change more than those under trial conditions (b), (d) and (e).

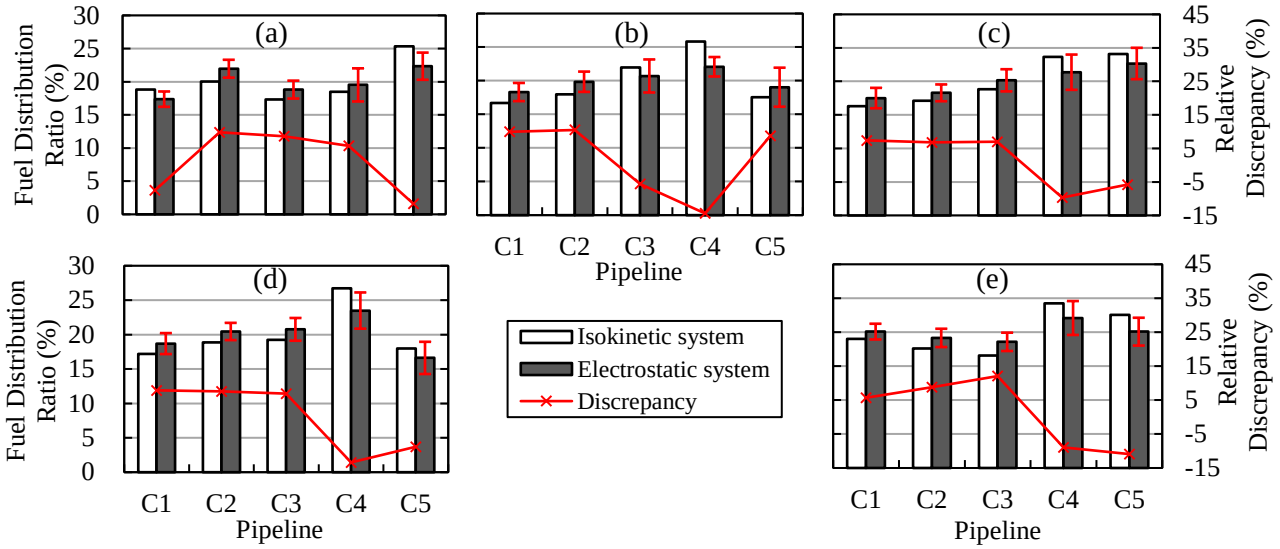

Fig. 13. PF distribution in the five primary air pipes under five different flow conditions.

V. CONCLUSIONS

The developed instrumentation system with five sensing heads has been implemented and installed on a 600 MW boiler unit of a commercial power plant. The on-plant comparison trials of the developed system and the isokinetic sampling equipment were conducted under five operating conditions after a series of calibration tests. The results from the comparison trials have demonstrated that effective and reliable mass flow distribution and velocity measurement of PF between the primary air pipes of the same mill is realized under typical industrial conditions. The results have indicated that the maximum relative deviation of velocities between the PF and the conveying air is 4.73% and the mean relative error of the measured PF mass flow rate is less than 2.54%. The relative discrepancy in mass flow distribution measurements between the developed system and the isokinetic method is no greater than ±15%, and the absolute deviations of mass flow distribution for all the primary pipes in the trials are within the range of 7.3% to 10.2%. While the relative discrepancy in PF velocity measurement between the two methods is no greater than ±5%, and the averaged absolute deviation of the PF velocities of the five primary pipes is between 2.7% and 6.0%. The proposed measurement system has clear advantages over the isokinetic sampling and existing commercial products, including non-invasiveness to the flow, on-line continuous measurement, low maintenance requirements, and passive measurement. It is

envisioned that the deployment of the system will enable the plant operators to achieve on-line continuous monitoring of fuel distribution between primary air pipes of the same mill and allow the plant operators to control and optimize the fuel supply under variable operating conditions.

ACKNOWLEDGMENT

Acknowledgments are made to the National Natural Science Foundation of China (No. 61603135), Chinese Ministry of Education (No. B13009) and the Fundamental Research Funds for the Central Universities from North China Electrical Power University (2016MS40) for funding this research. The authors would also like to thank technical staff at Guodian Changzhou Generating Co., Ltd and Xi'an Thermal Power Research Institute Co., Ltd, for their assistance during the on-plant trials.

REFERENCES

[1] International Energy Agency, Coal Medium-Term Market Report 2014, Organization for Economic Co-operation and Development (OECD), 2014.

[2] Y. Zheng and Q. Liu, "Review of techniques for the mass flow rate measurement of pneumatically conveyed solids," *Measurement*, vol. 44, pp. 589–604, 2011.

[3] Department of Trade and Industry (DTI). Multiphase flow technologies in coal-fired power plants, Technical Report, London, 2004.

[4] C. Xu, S. Wang, G. Tang, D. Yang, and B. Zhou, "Sensing characteristics of electrostatic inductive sensor for flow parameters measurement of pneumatically conveyed particles," *J. Electrost.*, vol. 65, pp. 582–92, 2007.

[5] J. B. Gajewski, "Electrostatic nonintrusive method for measuring the electric charge, mass flow rate, and velocity of particulates in the two phase gas–solid pipe flows—Its only or as many as 50 years of historical evolution," *IEEE Trans. Ind. Appl.*, vol. 44, no. 5, pp. 1418–1430, 2008.

[6] Y. Yan, B. Byrne, S. Woodhead, and J. Coulthard, “Velocity measurement of pneumatically conveyed solids using electrodynamic sensors,” *Meas. Sci. Technol.*, vol. 6, pp. 515–537, 1995.

[7] W. Zhang, C. Wang and Y. Wang, “Parameter selection in cross-correlation-based velocimetry using cicular electrostatic sensors,” *IEEE Trans. Instrum. Meas.*, vol. 59, no. 5, pp. 1268–1275, 2010.

[8] J. B. Gajewski, “Accuracy of cross correlation velocity measurements in two-phase gas–solid flows,” *Flow Meas. Instrum.*, vol. 30, pp. 133–137, 2013.

[9] C. Wang, J. Zhang, W. Gao, H. Ding and W. Wu, “Cross-correlation focus method with an electrostatic sensor array for local particle velocity measurement in dilute gas–solid two-phase flow,” *Meas. Sci. Technol.*, vol. 26, no. 10, 115301, 10pp, 2015.

[10] Y. Yan, B. Byrne, and J. Coulthard, “Sensing field homogeneity in mass flow rate measurement of pneumatically conveyed solids,” *Flow Meas. Instrum.*, vol. 8, pp. 115–119, 1995.

[11] Y. Yan, “Mass flow measurement of bulk solids in pneumatic pipelines,” *Meas. Sci. Technol.*, vol. 7, pp. 1687–1706, 1996.

[12] X. Qian and Y. Yan, “Flow measurement of biomass and blended biomass fuels in pneumatic conveying pipelines using electrostatic sensor-arrays,” *IEEE Trans. Instrum. Meas.*, vol. 61, no. 5, pp. 1343–1352, 2012.

[13] J. Li, M. Kong, C. Xu, S. Wang, Y. Fan, “An Integrated instrumentation system for velocity, concentration and mass flow rate measurement of solid particles based on electrostatic and capacitance sensors,” *Sensors* (Basel), vol. 15, no. 12, pp. 31023–31035, 2015.

[14] J. Zhang, “Air-solids flow measurement using electrostatic techniques,” in *Electrostatics*, H. Canbolat, Ed. Rijeka, Croatia: InTech, pp. 61–80, 2012.

[15] X. Qian, X. Huang, Y. Hu, and Y. Yan, “Pulverized coal flow metering on a full-scale power plant using electrostatic sensor arrays,” *Flow Meas. Instrum.*, vol. 40, pp. 185–191, 2014.

[16] B. Jurjevčič, A. Senegačnik, B. Drobinč, and I. Kuštrin, “The characterization of pulverized-coal pneumatic transport using an array of intrusive electrostatic sensors,” *IEEE Trans. Instrum. Meas.*, vol. 64, no. 12, pp. 3434–3443, 2015.

[17] X. Qian, X. Huang, Y. Hu and Yong Yan, “Measurement of the mass flow distribution of pulverized coal in primary air pipes using electrostatic sensing techniques,” in *Proc. IEEE I2MTC*, Taipei, Taiwan, pp. 488–492, May 23–26, 2015.